Advances in Nanocomposite Research 2 (2015) 19-30

Semnan University

Advances in Nanocomposite Research

Journal homepage: http://ANCR.journals.semnan.ac.ir

Designing of Plaster of Paris (PP) Containing Poly (vinyl alcohol) -g-Poly (2-Hydroxyethyl methacrylate-co-acrylic acid)(PVA-g-PHEMA-co-AA) Nanocomposites: Preparation, Characterization and Study of Physicochemical Behavior

Seeta Shukla [a], A.K.Bajpai[a*]

[a]*Bose Memorial Research Laboratory, Department of Chemistry, Government Autonomous Science College , Jabalpur (MP) 482001,India*

PAPER INFO.

History:
Received 30 June 2014
Revised 17 Nov. 2014
Accepted 10 Dec. 2014

Keywords:
Nanocomposites;
polymer;
mechanical properties;
biocompatibility;

A B S T R A C T

In the present work plaster of paris containing polymer-based nanocomposites were prepared through chemical crosslinking and graft copolymerization of 2-hydroxyethyl methacrylate (HEMA) and acrylic acid (AA) on to polyvinyl alcohol (PVA) in the presence of ethylene glycol dimethacrylate (EGDMA) as crosslinker and potassium persulphate (KPS) and potassium metabisulphite (MBS) as redox components. The structure of so prepared copolymers was confirmed by Fourier transform infrared (FTIR) spectroscopy while morphology was examined using scanning electron microscopy (SEM) analysis.
The nanocomposites were found to show good mechanical properties as evident from the obtained experimental data. The maximum and minimum compressive strength of nanocomposites were found to be 29.5 (MPa) and 4.02 (MPa), respectively whereas the maximum and minimum modulus were found to be 200 (MPa) and 34 (MPa). The water sorption behavior was found to be dependent on chemical composition of the nanocomposite matrix. The porosity of composite varied between 33 to 57%. The in vitroblood compatibility of the nanocomposite indicated that the adsorption of bovine serum albumin (BSA) varied from 0.015 to 0.047 mg g^{-1}, the percentage haemolysis was between 12.3 to 23.7% and the weights of blood clot formed on the composite surfaces were found in the range 13 to 37 mg

1. Introduction

Bionanocomposites are useful materials and their extraordinary versatility stems from the large selection of biopolymers and fillers available to researchers [1]. Bone is an amazing and a true nanocomposite and it is an excellent example of a dynamic tissue, since it has a unique capability of self-regenerating or self-remodeling to a certain extent throughout the life without leaving a scar[2].

Bone fractures and damages are serious health problems in all day clinical work. Replacement of extensive local bone loss is a significant clinical challenge. Bone grafts provide mechanical or structural support, fill defective gaps, and enhance bone tissue formation. There are a variety of bone grafting methodologies available that includes autografting, allografting, xenografting, and alloplastic or synthetic bone grafting, to manage this problem but each with their own advantages and disadvantages [3, 4]. For more than a century research has been perused trying to find a suitable

‡Corresponding author: Email: akbmrl@yahoo.co.in

material to repair or replace bone segments, either by “Autograft” which is clearly osteogenic, and is considered as a limited supply especially when it is used in children as a bone graft, or by “Allograft” which is demonstrated lower osteogenic capacity and it is slower than the new bone formation [5].

A variety of biomaterials have been investigated as bone graft substitutes, such as calcium sulfate hemihydrates or Plaster of Paris (PP) which is a calcium sulphate based compound and classified as bioactive material [6]. It is resorbed and replaced with bone during the healing process. It is composed of biocompatible and osteoconductive materials that facilitate the in growth of blood vessels and osteogenic cells [7, 8]. It is a bioactive osteoconductor due to its high level of biocompatibility and appropriate degradation rate [9]. PP is a ceramic material and has poor mechanical properties.

In the present work the authors have tried to develop a novel calcium sulphate-based nanocomposite in which the calcium sulphate hemihydrates (CSH) is encapsulated in a biodegradable and biocompatible polymer matrix, in order to retain the structural integrity and decrease the bioresorption rate in bone regeneration applications [10-12].

Two polymers were employed to realize this system: HEMA and AA, both of which are well known in biotechnological and drug delivery applications. However, the drawback of its rapid dissolution has been overcome by its polymerization either with less hydrophilic or hydrophobic monomers in presence of organic crosslinkers to form copolymers of tunable physicochemical properties [13]. It has also been established that polyacrylic acid does not only have property to adhere to tooth mineral or bone, but it could also be applied as pH responsive biomaterials [14, 15].

Recently, numerous nanocomposites based on PHEMA as polymeric matrix have been reported [16, 17]. HEMA is a favorable biomaterial because of its excellent biocompatibility and physicochemical properties similar to those of living tissues. It also exhibits good chemical and hydrolytic stability and good tolerance for entrapped cells [18]. PVA is a hydrophilic polymer possessing high permeability to small molecules and has been extensively applied in various biomedical applications.

2. Experimental

2.1.Materials

AA used as a monomer (E. Merck, India) was freed from inhibitor by washing with H_2SO_4 and NaOHand finally with distilled water followed by vacuum distillation. Plaster of paris (Medical grade) was supplied by E. Merck. Polyvinyl alcohol (Mol.wt 14000 Da, 98% hydrolyzed) was purchased from E.Merck, India and used without any pretreatment. HEMA was obtained from Sigma Aldrich Co. USA and freed from the inhibitor by prescribed method. The crosslinker used in polymerization was EGDMA obtained from Merck (Germany) and used as received. KPS and MBS obtained from Loba Chemicals India were employed as polymerization activator and initiator, respectively. Ethylene glycol (EG) (Merck, India) was used as a cosolvent. All chemicals were of analytical grade and doubly distilled water was used throughout the experiments.

2.2. Methodology

2.2.1. Purification of Monomer

Due to poor stability of HEMA, high purity of the monomer is essentially required in hydrogels synthesis as the presence of impurities may greatly affect the swelling characteristics of the end polymer. The HEMA was purified by a method reported in the literature [19].

2.2.2. Preparation of PP-poly (HEMA-co-AA) Nanocomposites

In order to achieve the desired polymer matrix, a free radical initiated polymerization method was adopted [20, 21]. In brief, 10 mL PVA solution (10% w/v) was taken with 2.132 g purified HEMA (2 hydroxyethyl methacrylate) monomer in a Petri dish. Then, ethylene glycol (4.44 g) as a co-solvent, EGDMA (0.209 g) as a crosslinker, and PP (4.0 g) were added to this mixture. For initiating polymerization reaction, a redox couple comprising of 1 mL each of degassed solutions of potassium persulphate (10 mg/10 mL) and potassium metabisulphite (90 mg/10 mL) were added to the reaction mixture and polymerization was allowed to proceed for 24 h at room temperature, to obtain a slab of the hydrogel. The manufacturing process of these scaffolds is shown inFig. 1.

2.3 Characterization

2.3.1 Mechanism of Grafting

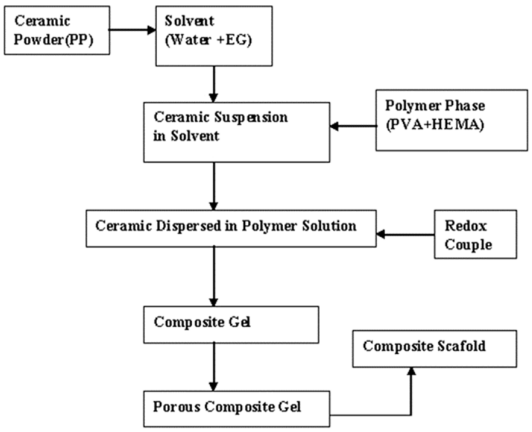

Fig. 1. Schematic diagram for the preparation of nanocomposites

The free radicals generated via the redox reaction between the KPS and MBS add onto the PVA macromolecule and generate macroradicals by abstraction of hydrogen atoms. Now the HEMA and AA monomer molecules add on to the PVA macroradicals and propagate the grafted copolymer macrochains which are eventually terminated by either normal unimolecular or bimolecular modes. The whole scheme of reactions has been presented in Fig. 2. It is also worthy to mention that from this mechanistic consideration the present grafted copolymer hydrogel may be coined as semi interpenetrating polymer network (IPN).

2.3.1 FTIR Studies

FTIR studies of the powdered specimens were recorded on a Perkin-Elmer (1000 Paragon, Shimadzu) spectrophotometer. Prior to analysis, KBr pellets were prepared by mixing 1:10 of sample: KBr (wt/wt) followed by uniaxillary pressing the powders under vacuum. The spectra were obtained between 4400 cm^{-1} to 450 cm^{-1} at 2 cm^{-1} resolution.

2.3.2 XRD Studies

The XRD apparatus (Philips PW1820 powder diffractometer) was used to determine the crystallinity and phase content of PP-poly (HEMA-co-AA) composites. The diffraction data were collected from 2° to 60°, 2θ values with a step size of 0.02° and counting time of 2 s step−1 at λ i.e., 1.54 A°.

2.3.3 Scanning Electron Microscopy

For examining the morphology of the prepared nanocomposites SEM was carried out on STEREO SCAN, 430, Leica SEM, USA.

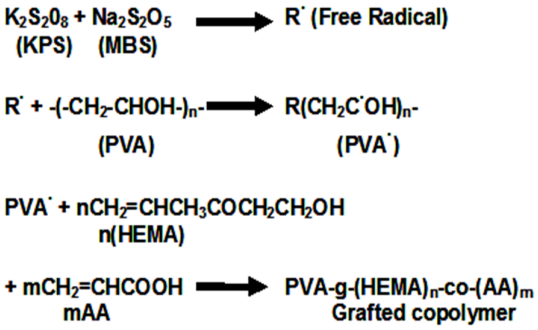

Fig. 2. The reaction scheme showing the graft copolymerization of HEMA-co-AA chains onto the PVA molecule.

2.3.4 Transmission Electron Microscopy (TEM) Studies

The size and morphology of the nanocomposites were determined by TEM analysis performed on Morgagni 268-D transmission electron microscope with an accelerating voltage of 80.0 kV. The samples for TEM measurements were prepared by dispersing a drop of the sample suspensions on Formvar-coated C grids.

2.3.5 Water Sorption Measurements

The extent of swelling was determined by a conventional gravimetric procedure as reported in the literature [22]. The swelling ratio was calculated by the Equation 1,

$$Swelling\ Ratio = \frac{Weight\ of\ Swollen\ gel}{Weight\ of\ Dry\ gel} \quad (1)$$

2.3.6 Porosity Determination

The apparent porosity of a porous scaffold can influence its mechanical strength, permeability, and presence of structural defects [23]. In the present work, the porosity was determined by the method reported in the literature [24]. In brief, the known volume and weight of the samples noted as Vo and Wo, respectively were immersed into the dehydrated alcohol for 48 h until absorbing dehydrated alcohol saturated the samples. The weight gained by the sample is measured as W_1. Finally the porosity (P) of the open pores in the composites were evaluated using the formula given in Equation 2,

$$P = \frac{W1-W0}{pV0} \quad (2)$$

Where **p** is the density of the dehydrated alcohol.

2.3.7 Blood Compatibility

Certain test procedures have been developed and they need to be employed to judge the haemo-friendly nature of the materials.

2.3.7.1 Protein (BSA) adsorption

The adsorption of BSA onto the prepared nanocomposites was performed by the batch process as reported elsewhere [25]. A known volume of protein solution of definite concentration is mildly shaken with the polymer composite matrix and the reaming concentration of protein was monitored in the solution spetrophotometrically. The amount of the adsorbed protein was calculated with the help of the following mass balance equation, .

$$\textit{Adsorbed amount (mg m}^{-2}\textit{) } A = \frac{(\mathrm{Co}-\mathrm{Co}).\mathrm{V}}{\mathrm{A}} \qquad (3)$$

Where Co and Ca being the concentrations of protein solution (mg per mL) before and after adsorption, respectively. V is the volume of the protein solution and A is the geometrical surface area of the adsorbent which was calculated with the help of its dimensions.

2.3.7.2 Clot formation test

The antithrombogenic potential of the composite surfaces may be judged by the blood clot formation test as described elsewhere [26]. In brief, the PP-polymer composites are equilibrated with saline water (0.9% w/v NaCl) for 72 h in a constant temperature bath. To these swollen composites was added 0.5 mL of acid citrate dextrose (ACD) blood followed by the addition of 0.03 mL of $CaCl_2$ solution (4 M) to start the thrombus formation. The reaction was stopped by adding 4.0 mL of deionized water and the thrombus formed is separated by soaking in water for 10 min at room temperature and then fixed in 36% formaldehyde solution (2.0 mL) for another 10 min. The fixed clot is placed in water for 10 min and after drying its weight is recorded

2.3.7.3 % Hemolysis tests

Hemolysis experiments were performed on the surfaces of the prepared composites as described elsewhere [27]. In a typical experiment, a dry composite disc is equilibrated in normal saline water (0.9% NaCl solution) for 24 h at 37◦C for 24 h and human ACD blood (0.25 mL) was added into the gels. After 20 min, 2.0 mL of saline water was added on the surface to stop haemolysis and the sample is incubated for 60 min at 37◦C. Positive and negative controls were obtained by adding 0.025 mL of human ACD blood and saline solution, respectively to 2.0 mL of distilled water. Incubated samples were centrifuged for 45 min, the supernatant was taken and its absorbance was recorded on a spectrophotometer at 545 nm. The percent of haemolysis was calculated using the following relationship,

$$\%\ \textit{Haemolysis} = \frac{A\ test\ sample - A\ (-) sample}{A\ (+) sample - A\ (-) sample} \qquad (4)$$

Where A = Absorbance.

3. Results and Discussion

3.1. FTIR Studies

The FTIR spectra of native PP and PP-poly (HEMA-co-AA) composite are shown in Fig. 3**.** The strong bands appeared in the region 1080 to 1150 cm^{-1} and also medium to strong bands between 580 to 670 cm^{-1} clearly show the presence of the sulphate ions (SO_4^{2-}). The presence of hydroxyl bands in the range 3700 to 3100 cm^{-1} is convenient for distinguishing the different hydrates in the system $CaSO_4$-H_2O. The three types of $CaSO_4$: gypsum, hemihydrates and anhydrite, are easily identified just by the differences around 3500 cm^{-1} and by the different splitting of the peak around 1620 cm^{-1} [28]. The peaks that appear at 1178 cm^{-1} and 1035 cm^{-1} are for the S=O asymmetric and symmetric stretching vibration respectively[29].

The FTIR spectra clearly show the presence of PVA as evident from a broad band appearing at 3418 cm^{-1} (due to hydrogen bonded hydroxyls); methylene groups at 2925 cm^{-1} (asymmetric

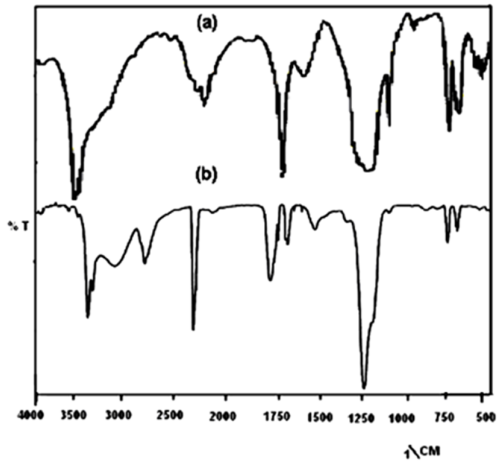

Fig-3 FTIR spectra of (a) native plaster of paris, and (b) PP-poly (HEMA-co-AA) composite.

stretching, CH_2) and at 2854 cm^{-1} (symmetric stretching, CH_2); and carboxyl groups at 1595 cm^{-1}(asymmetric stretching of -COO-); and 1460 cm^{-1} (symmetric stretching of -COO-) [30]. The spectral peak of C=O vibration at 1724 cm^{-1}suggests that the PAA were firmly introduced into the composite system .The characteristic absorption peak of C=C at 1676 cm^{-1} indicate that the vinyl groups were successfully grafted into the nanocomposite [31]. Bands at 1457 (C–H), 1410, 1170, and 1070 cm^{-1} indicated the existence of poly (acrylic acid) chains [32]. The presence of HEMA in PP-poly (HEMA-co-AA) nanocomposite is confirmed by the observed absorption bands at 1700 and 1072 cm^{-1}, which refer to C=O and C-O stretching of the ester groups in PHEMA [33].

3.2 XRD Studies

The XRD spectra of native PP and prepared nanocomposites are shown in Fig. 4 (a) and (b), respectively. The spectra (a) exhibits several characteristic sharp peaks at 2θ values of about 15°, 25°, 30° and 32°, respectively of varying intensities were detected which clearly confirm the presence of well crystalline PP phase. The XRD spectra (b) of PP-poly (HEMA-co-AA) composite show slight broadening of the peaks suggesting for a decrease in crystallinity of PP because of incorporation of organic polymer matrix. The prominent XRD peaks at about 27° and 38° of almost equal intensities show well crystalline nature of PP even in the nanocomposite also. The formation of these nanocomposites depends on the structure of the host material itself, the charge density on the surface, the method of preparation, and the type of organic polymers. The small expansion upon intercalation could only be explained by a single linear extension conformation of PAA molecules [34]. In results a peak around 20° which is corresponds to the (101) plane of the PVA crystal [35]. The mean grain size was calculated using Debye-Scherer formula (36, 37) as shown in Equation (5),

$$d = \frac{k\lambda}{\beta \cos\theta} \qquad (5)$$

Where dis mean grain size, kis the shape factor (0.9), β is broadening of the diffraction angle and λ is diffraction wavelength (1.54 A°). The estimated average grain size of PP was found to be 7.77 nm. The % crystallinity has been calculated for the irradiated PP-poly (HEMA-co-AA) composites

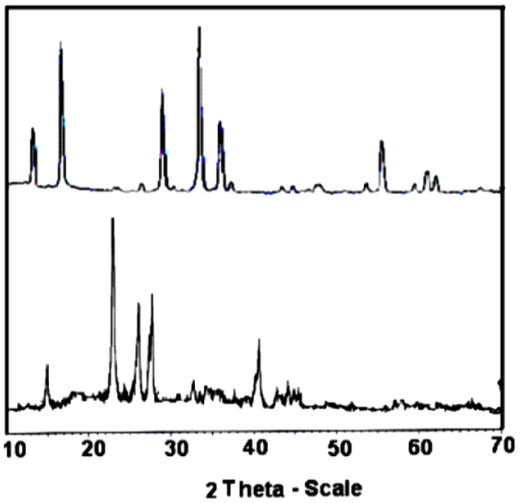

Fig-4. XRD of (a) native plaster of paris, and (b) PP-poly (HEMA-co-AA) composite.

usingthe following expression given in literature [38],

$$\% \text{ Crystality} = I_c/I_a + k.I_a \qquad (6)$$

Where I_c and I_a are the integrated intensities of crystalline and amorphous peaks, respectively, K is a constant taken as unity [39]. Areas of the peaks were determined by the "cut and weight method". The relation between integrated intensities and area of crystalline and amorphous peaks has been evaluated from the literature [40]. It has been found that the % crystallinity of the composite containing 2.132 g HEMA and 4.0 g PP is calculated to be about 10.32.

3.3 SEM Studies

The SEM images of the composites are shown in Figure 5 which clearly shows that the composite surface is highly porous in nature and PP crystals are present as clusters of cylindrical shape. It is clear from the two micrograph images that the prepared composites exhibit quite similar morphology as natural bone. The size of the

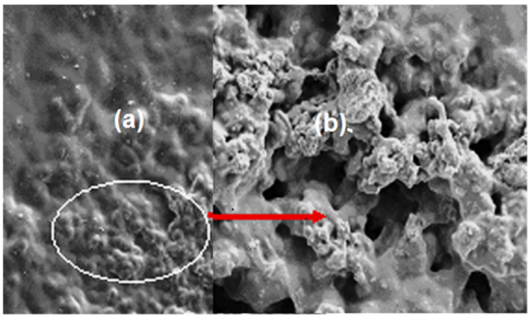

Fig. 5. The SEM images of PP-poly (HEMA-co-AA) nanocomposite.

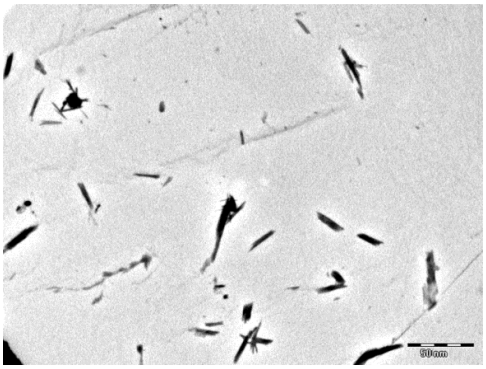

Fig. 6. The TEM image of PP-poly (HEMA-co-AA) nanocomposite.

aggregated crystals varies in the range 10 to 30μm having an average width of 5 μm. The size of the pores varies in the range 3 to 20 μm as indicated by arrows in the same Figure.

3.4 TEM Studies

In order to investigate the size and morphology of prepared nanocomposites TEM images were recorded as shown in Figure 6. It is clear from the image that the PP molecules are present as aggregated needle shaped fibrils of nanodimension.

3.5 Mechanical Testing

To examine the mechanical properties of the prepared nanocomposites compression tests of the specimens were conducted in both dry and wet conditions. The results summarized in Table 1 clearly indicate that the maximum and minimum compressive strength of nanocomposites were found to be 29.5 (MPa) and 4.02 (MPa), respectively whereas the maximum and minimum modulus were found to be 200 (MPa) and 34 (MPa). The data are in good agreement with those of the trabecular bone which is reported to have

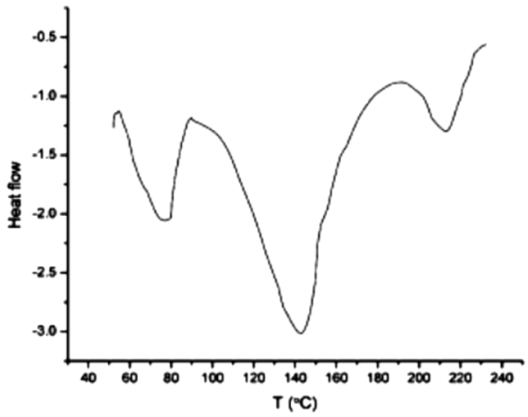

Fig.7 (a) Effect of PVA content on swelling ratio of the nanocomposite.(b) Effect of PHEMA content on swelling ratio of the nanocomposite

compressive strength and Young's modulus ranging between 2–10 MPa and 50–100 MPa, respectively [41]. It is also clear that the mechanical strength in wet condition is not very much less than that in dry condition.

3.6 Differential Scanning Calorimetry (DSC) Studies

Thermal characterization of the prepared PP-poly (HEMA-co-AA) nanocomposite has beenperformed by recording DSC thermogram as shown in Fig. 7. The results obtain from DSC thermogram shows the combined thermal features of components of nanocomposites, i.e. PVA,PHEMA, PAA and PP. It is clear from the thermogram that a very minor inflexion appears at 72.4 °C, which may be assigned to the glasstransition temperature of PVA. Another notable occurrence of relatively sharper endotherm around 152 °C appears significantly higher than the reported value of 113°C [42].The observed shift in

Table 1. Data showing the compressive strength and modulus of PP-poly (HEMA-co-AA) nanocomposites of different compositions

PVA (wt %)	PP (wt %)	HEMA (wt %)	EGDMA (wt %)	AA (wt %)	Compressive strength (MPa)		Modulus (MPa)	
					In dry	In wet	In dry	In wet
5.59	44.76	23.85	2.33	23.44	4.02	2.97	34	30
22.86	36.57	19.49	1.91	19.15	6.20	5.00	52	44
13.44	26.89	28.67	2.81	28.17	18.0	14.20	180	158
9.58	47.91	20.42	2.00	20.07	20.0	17.6	100	90
12.75	51.03	6.80	2.66	26.7	11.30	10.2	110	102
١١,٢٣	٤٤,٩٢	١٧,٩٦	٢,٣٤	٢٣,٥٣	12.67	10.41	135	123
10.01	40.07	26.82	2.09	20.98	14.0	11.97	200	179
10.71	42.86	22.84	1.11	22.45	8.70	5.34	56	42
10.36	41.46	22.10	4.34	21.71	7.40	5.36	120	111
11.92	47.70	25.42	2.49	12.45	26.2	23.52	160	149
10.03	40.15	21.40	2.09	26.30	29.5	26.85	178	163

T_g to higher temperature may be attributed to the crosslinking of the PHEMA segments by EGDMA.The DSC thermogram shows a sharp endotherm around 222 °C which may be attributed to the first decomposition of PAA.The sharp endotherm also implies enhanced crystallinity of the nanocomposite which could be attributed to impregnation of crystalline PP into the polymer matrix.

3.7 Swelling Behavior of Composites

Realizing the significance of water sorption capacity of a material, the PP-poly (HEMA-co-AA) composites have been investigated for water sorption capacity and the influence of chemical composition of the composites on their water intake has been investigated as discussed below.

3.7.1. Effect of PVA

In the present study the swelling ratio of the PP-poly (HEMA-co-AA) composites was investigated by varying the amount of PVA in the range 0.5 g to 2.0 g in the feed mixture of the composite. The results are shown in Figure 8 (a), which implies that initially the swelling ratio increases while in later course it constantly decreases. The results also reveal that at higher amounts of PVA the equilibrium swelling is attained earlier in comparison to the composite with low PVA content. The results can be explained by the fact that an increasing proportion of PVA results in greater hydration of its chains because of the hydrophilic nature of the PVA. However, beyond an optimum amount (1.0 g) the decrease observed in the swelling ratio is due to much greater density of the composite which inhibits diffusion of penetrant water molecules into the composite matrix. The arrival of equilibrium swelling of hydrogel at earlier times at higher PVA concentration may be attributed to the fact that at higher PVA concentration relaxation of PVA chains becomes difficult and this obviously leads tomuch slower penetration of water molecules which brings about in an early arrival of equilibrium swelling of the composites.

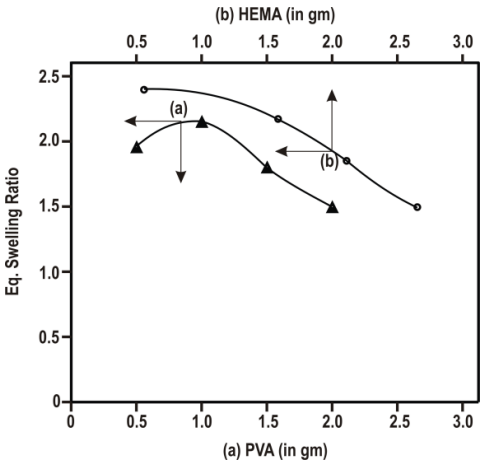

Fig.8 (a)Influence of PP content on swelling ratio of the nanocomposite (b) Effect of crosslinker (EGDMA) content on the swelling ratio.

3.7.2. Effect of PHEMA

The influence of PHEMA content of the nanocomposite on its swelling behavior has been investigated by varying its concentration in the feed mixture in the range of 0.533 g to 2.678 g. The results are shown in Figure 8 (b) which clearly indicates a constant fall in the water sorption capacity with increasing PHEMA content. This can be explained on the basis of Flory's ionic swelling theory [43]. According to this theory, the hydroxyl group of HEMA does not dissociate and the amount of dissociated ions inside the polymeric gel decreases with increasing concentration of HEMA. This consequently results in a decrease in the osmotic pressure difference between the polymeric gel and the external solution. In addition, since the hydroxyl groups are quite hydrophilic in nature and may subsequently produce hydrogen bonds between two neighboring chains that ultimately causes the network to shrink.

3.7.3. Effect of PP

The results of PP impregnation shown in Figure9(a) clearly reveal that the swelling ratio constantly increases with increasing PP content in the composite. The results are quite expected and may be explained by the fact that due to higher hydrophilicity of PP, its increasing amount in the composite results in a higher water sorption by the

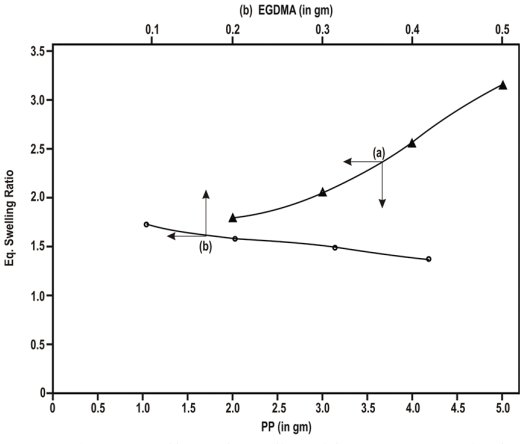

Fig.9 (a) Effect of acrylic acid (AA) content in the nanocomposite on swelling ratio.(b) Effect of pH of the swelling bath on PP-poly (HEMA-co-AA)nanocomposite.

composite. Alternatively, the increasing polymer-PP interactions with increasing amount of PP lead to stabilize the polymer chains so that the swelling ratio increases.

3.7.4. Effect of EGDMA

The crosslinking agent employed in this study was EGDMA, a known hydrophobic crosslinker. The addition of crosslinker not only enhances the degree of crosslinking but also decreases the glass transition temperature (Tg). In this study, the effect of crosslinker content in the composite on its swelling capacity has been studied by varying amount of EGDMA ranging from 0.104 g to 0.419 g. The results shown in Figure 9 (b) reveal that with increasing content of EGDMA the crosslink density of the network increases, which results in narrow size of the network pores. This clearly slows down the diffusion of water molecules into the composite [44] and consequently results in a suppressed swelling.

3.7.5. Effect of AA

In the present study the effect of AA on the swelling ratio of the nanocomposite was investigated by varying the AA in the concentration range 1.044 g to 2.620 g in the feed mixture of the composite. The results are shown in Figure 10(a), which indicates that the swelling ratio increases with an increase in AA in the composite. The observed findings may be explained by the fact that on increasing AA content in the composite, the composite acquires increasing anionic charge due to dissociable –COOH groups, which results in expansion of the network due to interchain

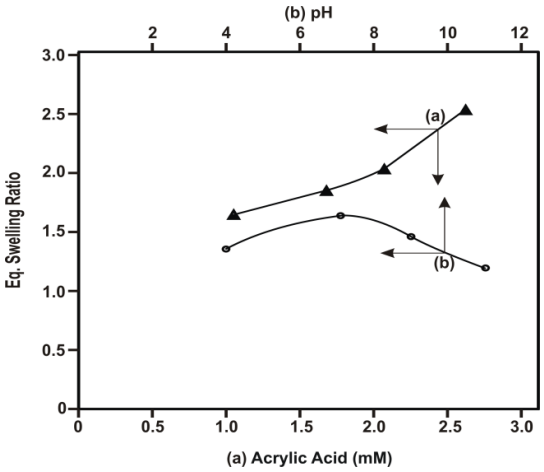

Fig.10 Effect of simulated biological fluids on swelling ration of the PP-poly (HEMA-co-AA) nanocomposite.

repulsions between $–COO^-$ charges. Another reason for the observed decrease in swelling ratio may be attributed to (a) preferential homopolymerization over graft copolymerization, (b) increase in viscosity of the medium which hinders the movement of free radicals and monomer molecules, (c) the enhanced chance of chain transfer to monomer molecules [45].

3.7.6. Effect of pH

In the present investigation the effect of pH has been investigated in the range 4.0 to 11.0 and the results are depicted in Figure 10 (b). It is clear from the Figure that the equilibrium swelling increases with increasing pH of the swelling medium. This can be explained by the fact that with increasing pH of the swelling medium the poly acrylic acid segments of the copolymer undergo partial hydrolysis and consequently produce anionic charged centers along the co-polymeric chains. These polyelectrolyte chains cause repulsions between the macromolecular chains and thus widen the free volumes within the composite network which obviously enhances their water sorption quality. However, beyond pH 7.4, the swelling ratio decreases, which may be due to the decreasing ionic osmotic pressure as predicted by the well-known Donnan membrane theory [46].

3.7.7. Effect of Temperature

The effect of temperature on the degree of water sorption has been investigated by carrying out water sorption experiments in the range 10 to 40°C. The results clearly indicate that the swelling ratio markedly increases up to 30°C temperature of the swelling medium, while beyond it a fall in swelling is observed. The results may be explained by the fact that when the temperature is increased, both the segmental mobility of the composite chains and diffusion of water molecules into the matrix increase which obviously results in greater swelling. However, beyond 30°C, a decrease in equilibrium swelling may be explained due to the breaking up of hydrogen bonds between water molecules and polymer chains.

3.8 Stability in Biofluids

In practical biomedical application, biomaterials often come in contact with physiological fluids for an intended period of time depending on the end use of the material. The effect of biological fluids has been examined by performing swelling experiments in the presence of Urea, D-glucose (5% w/v), potassium iodide (15%

w/v) and in physiological fluids such as saline water (0.9% w/v) and artificial urine. The results are summarized in Figure 11, which clearly show that the presence of solute suppresses the swelling ratio due to a decrease in osmotic pressure of external solution [47].

3.9 Percent Porosity

The measured porosity values of the PP-poly (HEMA-co-AA) composites are given in **Table 2**,which reveal fact that as the amount of cross linker is increased in the feed mixture, the porosity becomes low. The results are quite obvious since increased number of crosslinks make polymer network more compact which results in the lower mesh size and decreased porosity. It was found that the addition of PP results in more dense and thicker However the decrease in porosity observed with the increased amount of PAA in feed mixture is mainly due to the decrease in the PP/polymer ratio in the dispersed phase which in turns improves thesintering and porosity reduction [49]. As the amount of PVA is increased in the feed mixture porosity increases, this may be explained on the basis of the fact that PVA is a hydrophilic polymer and during the formation of matrix it lets the polymer network to swell in greater amount, which pore walls with lower porosity [48] as shown in Table 2. in turn results in greater pore size within the network and after drying the matrix, it yields greater porosity.

3.10 Blood Compatibility

In the present study, the adsorption of BSA onto swollen nanocomposites was determined and the results summarized in **Table 3** clearly indicate that the amount of BSA adsorbed constantly decreases with increasing PHEMA content of the composite. A decreasing protein adsorptionobviously implies for an increasing bloodconfirmed by the observed lower values of blood clots and percent haemolysis. The observed enhanced blood compatibility parameters may be attributed to thereason that increasing PHEMA content results in an enhanced hydrophilicity of the matrix which wouldresult in less adsorption of protein. In fact a largenumber of investigators have confirmed the observation that the composition and organization of the adsorbed protein layer can be varied by numerous factors

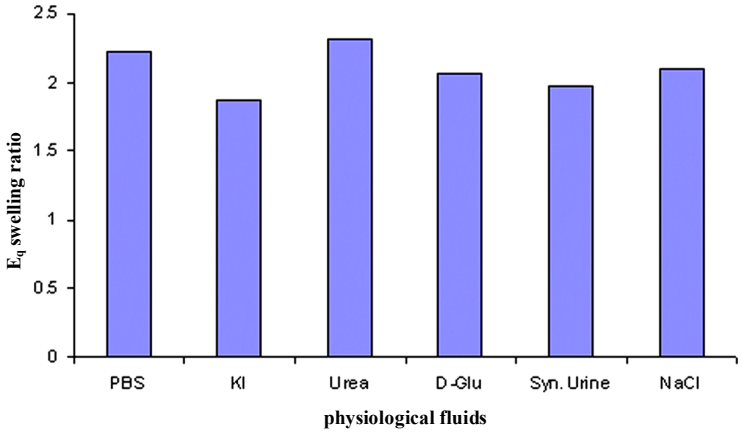

Fig11. Equilibrium swelling ratio of different physiological fluids.

Table 2. Data showing the percent porosity of PP-poly (HEMA-co-AA) nanocomposites of varying compositions

PVA (wt %)	PP (wt %)	HEMA (wt %)	EGDMA (wt %)	AA (wt %)	% Porosity
5.59	44.76	23.85	2.33	23.44	40
22.86	36.57	19.49	1.91	19.15	52
13.44	26.89	28.67	2.81	28.17	45
9.58	47.91	20.42	2.00	20.07	33
12.75	51.03	6.80	2.66	26.7	54
10.01	40.07	26.82	2.09	20.98	38
10.71	42.86	22.84	1.11	22.45	57
10.36	41.46	22.10	4.34	21.71	40
11.92	47.70	25.42	2.49	12.45	53
10.03	40.15	21.40	2.09	26.30	41

microphase separation and surface chemical functionality. As far as the chemistry of surface is confirmed, the effect of hydrophilic and hydrophobic groups of constituent chains on polymer surfaces has been found to play a key role in influencing protein adsorption and subsequent platelet adsorption to polymer surface [50]. Thus the above mentioned facts may be regarded as responsible factors for the protein adsorption, lower clot formation and decreased degree of haemolysis.

Another reason for the observed higher blood compatibility with increasing PHEMA content maybe attributed to the fact that at higher PHEMA content in the composite, phase separation becomesprominent and hydrophilic domains are formed on the gel surfaces. This obviously results in an exposure of hydrophilic and ionic groups to invading protein molecules and, therefore, the amount of adsorbed proteins decreases. The data summarized in Table 3 also indicate that increasing concentration of PAA in the gel brings about a fall in protein adsorption, clot formation and percent haemolysis. With increasing PAA content, the hydrophilicity of the gel surface increases which obviously results in lower amount of protein adsorption

The effect of increasing the crosslinker (EGDMA) concentration in the prepared composites on the amount of the clot formed was investigated by increases in its concentration in the range of 0.53 mM to 2.12 mM. The results summarized in Table 3 indicate an increase in the weight of the blood clot that formed with an increasing amount of the crosslinker. The results could be explained by the fact that because EGDMA is a hydrophobic crosslinker, its increasing content in the composite enhanced the hydrophobicity of the matrix, which eventually produced more blood clotting on the surface. For protein adsorption and percent haemolysis the observed results were consistent with blood clot formation test results and led us to conclude that a material surface showing resistance to fibrinogen adsorption may prove to be more blood compatible.

The influence of PVA on the blood compatibility of prepared composites has also been investigated by varying the amount of PVA in the feed mixture of the composite in the range 0.5 g to 2.0 g. The results summarized in Table 3 clearly show that with increasing PVA content in the gel the blood compatibility decreases which is clearly shown by the observed increased values of blood clot formed, percent haemolysis and adsorbed protein. The observed results are a little bit unusual as PVA is known to be a highly biocompatible polymer. The obtained findings may be attributed to the reason that with increasing amount of PVA, the intermolecular forces operative between PVA macromolecules also increase which results in a compact conformation of the molecule, thus exposing hydrophobic domains (back bone of PVA) to the invading protein molecules. This obviously results not only in greater protein adsorption but also in reduced hydrophilic nature of the gel which eventually results in a fall in the blood compatibility.One of the components of the composite is PP and its amount in the composite is expected to influence blood compatibility of the matrix. In order to examine it the concentration of PP powderwas varied in the range 2.0 g to 5.0 g and blood compatibility parameters were evaluated. The data summarized in Table 3 reveal that with increasing PP content, the blood compatibility decreases, i.e. all the three parameters increase. Thereason for the observed greater thrombogenicity ofthe composite is that the ionic groups of PP mayinteract with the blood

Table 3-Data showing the blood compatibility parameters of PP-poly (HEMA-co-AA) nanocomposites of varying compositions.

PVA (wt %)	PP (wt %)	HEMA (wt %)	EGDMA (wt %)	AA (wt %)	BSA adsorption [mg g^{-1}]	Percentage haemolysis	Blood clot formation [mg]
5.59	44.76	23.85	2.33	23.44	0.047	23.7	30
22.86	36.57	19.49	1.91	19.15	0.031	17.1	21
13.44	26.89	28.67	2.81	28.17	0.035	18.3	13
9.58	47.91	20.42	2.00	20.07	0.040	23.8	23
12.75	51.03	6.80	2.66	26.7	0.042	19.8	34
10.01	40.07	26.82	2.09	20.98	0.031	15.9	22
10.71	42.86	22.84	1.11	22.45	0.026	12.3	28
10.36	41.46	22.10	4.34	21.71	0.037	18.4	37
11.92	47.70	25.42	2.49	12.45	0.024	16.4	37
10.03	40.15	21.40	2.09	26.30	0.015	19.4	28

components and produce greater blood surface interactions. This is likely to cause an increase in thrombogenic behavior of the composite. The above discussion clearly reveal that a less crosslinked composite with more PAA and low PP content may prove to be greater biocompatible

4. Conclusions

In the present study, PP-poly (HEMA-co-AA) nanocomposites were successfully prepared by free radical polymerization of AA and HEMA in the presence of a crosslinker (EGDMA) and apreformed polymer (PVA) with plaster of Paris (PP) as inorganic component for potential use as bone replacement materials.

The FTIR spectra of the composite clearly mark the presence of Plaster of Paris (PP) and polymer components in the nanocomposite. The XRD studies confirm the nanosized mean grain size of the PP powder in native state as well as in the composites. DSC thermogram of the prepared composite revealed that composite is more thermally stable than the polymer matrix alone.

The SEM analysis of the composite indicates a porous type of surface having pore size in the range 3 to 20 μm whereas the TEM image clearly suggests for plaster of paris particles in nanodimension. The mechanical testing results showed that the chemical bonding of PP filler to polymer matrix had a distinct effect on the mechanical properties of the composites in both dry and wet conditions. The maximum and minimum compressive strength of nanocomposites were found to be 22 ± 13 (MPa) and 4.02 ± 2.34 (MPa) whereas the maximum and minimum modulus were found to be 56 ± 200 (MPa) and 34 ± 28 (MPa).

Swelling studies show the effect of composition on the swelling. It is found that as the PAA and PP contents increases, the swelling ratio also increases. The extent of swelling decreases with increasing amounts of HEMA and crosslinker.

References

1. Rohan A, Hule and Pochan DJ. Polymer Nanocomposites for Biomedical Applications. MRS Bulletin. 2007; 32: 354-358.
2. Boyle WJ, Simonet WS, and Lacey DL. Osteoclast differentiation and activation. Nature. 2003; 423: 337-342.
3. Zhang P, Hong Z, Yu T, Chen X, Jing X. In vivo mineralization and osteogenesis of nanocomposite scaffold of poly (lactide-co-glycolide) and hydroxyapatite surface-grafted with poly (L-lactide) Peibiao. Biomaterials. 2009; 30: 58-70.
4. Myerson MS, Neufeld SK, Uribe J. Fresh-frozen structural allografts in the foot and ankle. J. Bone Joint Surg. Am. 2005; 87**:** 113-120.
5. Oktar FN. Hydroxyapatite-TiO_2 composites. Materials Letters. 2006; 60: 2207.
6. Thomas MV, Puleo DA. Calcium sulfate: Properties and clinical applications. J. Biomed.Mater.Res. Part B- Appl. Biomaterl. 2009; 88: 597-610.
7. Panchbhavi VK. Synthetic bone grafting in foot and ankle surgery. Foot Ankle Clin. N Am. 2010; 15: 559-576.
8. Beardmore AA, Brooks DE, Wenke JC, Thomas DB. Effectiveness of Local Antibiotic Delivery with an Osteoinductive and Osteoconductive Bone-Graft Substitute J. Bone Joint Surg. Am. 2005; 87: 107-112.
9. Jang KH, Park RW, Kim IS. The Effect of Chitosan Bead Encapsulating Calcium Sulfate as an Injectable Bone Substitute on Consolidation in the Mandibular Distraction Osteogenesis of a Dog Model. Oral Maxillofac Surg. 2005; 63: 1753-1764.
10. Elkayar A, Elshazly Y, Assaadt M., Properties of Hydroxyapatite from Bovine Teeth Bone Tissue Regen. Insights. 2009; 2: 31-36.
11. D'Ayala GG, De Rosa A, Laurienzo P, Malinconico M. Development of a new calcium sulphate-based composite using alginate and chemically modified chitosan for bone regeneration. Biomed. Mater. Res. - Part A. 2007; 81: 811-820.
12. Wang P, Lee EJ, Park CS, Yoon BH, Shin DS, Kim HE, Koh YH, Park SH. Calcium Sulfate Hemihydrate Powders with a Controlled Morphology for Use as Bone Cement. J. Am. Ceramic Society. 2008; 91: 2039-2042.
13. Gils PS, Ray D, Mohanta GP, Manavalan R, Sahoo P. Designing of new Acrylic based macroporous superabsorbent polymer hydrogeland its suitability for drug delivery. Int. J. Pharmacy Pharmaceut. Sci.2009; 1: 43-54.
14. Miyazaki K, Horibe T, Antonucci JM, Takagi S, Chow LC. Polymeric calcium phosphate cements: analysis of reaction products and properties. Dent Mater. 1993; 9: 41-45.
15. Misra DN. Adsorption of low-molecular-weight sodium polyacrylate on hydroxyapatite. J. Dent. Res. 1993; 71: 1418-1422.
16. Horak D, Rittich B, Safar J, Spanova A, Lenfeld, J, Benes M. Properties of RNase A immobilized on magnetic Poly(2-hydroxyethyl methacrylate) microspheres. J. Biotechnol. Progr. 2001; 17: 447-452.
17. Flynn L, Dalton PD, Shoichet MS. Fiber templating of poly(2-hydroxyethyl methacrylate) for neural tissue engineering. Biomaterials. 2003; 24: 4265-4272.
18. Simonida LT, Edin HS, Jovanka MF. Biocompatible and bioadhesive hydrogels based on 2-hydroxyethyl methacrylate, monofunctional poly (alkylene glycol)s and itaconic acid. Polym Bull. 2006; 57: 691-702.
19. Bajpai AK, Kankane S.Evaluation of water sorption property and in vitro blood compatibility of poly(2-hydroxyethyl methacrylate) (PHEMA) based semi interpenetrating polymer networks (IPNs).J.Materl.Sci.: Mater.Med. 2008; 19: 1921-1933.

20. David N**,** Harald EN, Bersee andKrzysztof JK**.** The use of polyurethane scaffold forcartilage tissue engineering: potentials and limitations.Biomaterials.2006; 27: 1522-1534.
21. Bajpai AK, Shrivastava M.Water sorption dynamics of hydrophobic, ionizable copolymer gels. J. Sci. Ind. Res. 2001; 60: 131-140.
22. Mishra S, Bajpai R, Katare R, Bajpai AK. Preparation, characterization and microhardness study of semi interpenetrating polymer networks of polyvinyl alcohol and crosslinked polyacrylamide. J. Mater. Sci.: Mater. Med**.** 2006; 17: 1305-1313.
23. Bundela H, Bajpai AK. Designing of hydroxyapatite-gelatin based porous matrix as bone substitute: correlation with biocompatibility aspects.eXPRESS Polym. Lett. 2008; 2: 201-213.
24. Zhang Y, Zhang MJ. Synthesis and characterization of macroporous chitosan/calcium phosphate composite scaffolds for tissue engineering. J. Biomed. Mater. Res. 2001; 55: 304-312.
25. Bajpai AK.Blood protein adsorption onto macroporous semi-interpenetrating polymer networks (IPNs) of poly(ethylene glycol) (PEG) and poly(2-hydroxyethyl methacrylate) (PHEMA) and assessment of in vitro blood compatibility. Polym. Int. 2007; 56: 231-244.
26. Bajpai AK,Mishra DD. Dynamics of blood protein adsorption onto poly (2-hydroxyethyl methacrylate)-silica nanocomposites: Correlation with biocompatibility. J. Appl. Polymer Sci. 2008; 107: 541-553.
27. Bajpai AK, Saini R. Preparation and characterization of biocompatible spongy cryogels of poly (vinyl alcohol)-gelatin and study of water sorption behavior. Polym. Int. 2005; 54: 1233-1242.
28. Jr.-J.R. Dyer, Application of Absorption Spectroscopy of Organic Compounds, Oxford Press, London; 1984.
29. Bajpai AK, Singh R. Study of biomineralization of poly (vinyl alcohol)-based scaffolds using an alternate soaking approach. Polm. Int. 2007; 56: 557-568.
30. Wei F, Yang J, Gu FN, Gao L, Zhu JH. Direct synthesis of high quality cubic Ia3d mesoporous material under organosilane assisted. Micropor. Mesopor. Mater. 2010; 130: 266-273.
31. Spagnola C, Rodriguesa HA, Pereiraa GB, Fajardoa R, Rubiraa F, Muniza C. Superabsorbent hydrogel composite made of cellulose nanofibrils and chitosan-graft-poly(acrylic acid). Carbohydr. Polym. 2011; 87: 2038-2045.
32. Khanchaiyapoom K, Prachayawarakorn J. Physical and Dyeing Properties Using Natural Dyes of Degummed Silks (Bombyx mori) Grafted by 2-Hydroxyethyl Methacrylate . J. Metals, Materl. Minrl. 2008; 18: 237-240.
33. Mojumdar SC, Raki L. Preparation, thermal, spectral and microscopic studies of calcium silicate hydrate-poly (acrylic acid) nanocomposite materials. J. Thermal Analy Calorymetry. 2006; 85: 99-105.
34. Spanos N, Klepetsanis PG, Koutsoukos PG. Model Studies on the Interaction of Amino Acids with Biominerals: The Effect of L-Serine at the Hydroxyapatite-Water Interface J. Coll. Interf. Sci. 2006*;* 236: 260-265.
35. Rahaman MN (1995).Ceramics processing and sintering, (Marcel Dekker, New York), pp. 1-37.
36. Prabakaran K, Thamaraiselvi TV, Rajeswari S. Electrochemical Evaluation of Hydroxyapatite Reinforced Phosphoric Acid treated 316L stainless steel. Trends Biomater. Artif. Org. 2006; 19: 84-87.
37. Hussain R, Qadeer R, Ahmed M, Saleem M. X-Ray diffraction study of Heat-Treated Graphitized and Ungraphitized Carbon. Turk. J. Chem. 2000; 24: 177-183.
38. Johnson JEJ. X-ray diffraction studies of the crystallinity in polyethylene terephthalate J. Appl. Polym. Sci. 1959; 2: 205-209.
39. Ning Y. Determination of the crystallinity in different type poly (oxyethylene-styrene) block copolymers by x-ray diffraction method. Chinese J. Polym. Sci. 1989; 7: 315-321.
40. Tas AC. Preparation of Porous Bioceramics by a Simple PVA-Processing Route. Key Eng. Materl. 2004; 264: 2079-2082.
41. Shukla S. and Bajpai AK. A facile approach to design plaster of paris based polymer nanocomposites for possible use as bone implants.J. Macromol. Sci.- Part A: Pure Appl. Chem. 2010; 47: 849-860.
42. Flory PJ, Principle of Polymer Chemistry Cornell University Press, Ithaca, NY, 1953.
43. Bajpai AK, Mishra A. Preparation and characterization of tetracycline-loaded interpenetrating polymer networks of carboxymethyl cellulose and poly(acrylic acid): Water sorption and drug release study. Polym. Int. 2005; 54: 1347-1356.
44. Mohapatra R, Ray D, Swain AK, Pal TK, Sahoo PK. Release study of alfuzosin hydrochloride loaded to novel hydrogel p (HEMA-co-AA). J Appl Polym. Sci. 2008; 108: 380-386.
45. Spagnola C, Rodriguesa HA, Pereiraa GB, Fajardoa R, Rubiraa F, Muniza C. Superabsorbent hydrogel composite made of cellulose nanofibrils and chitosan-graft-poly (acrylic acid). Polymer. 2011; 87: 2038-2045.
46. Bajpai AK, Bajpai J, Soni SN. Preparation and characterization of electrically conductive composites of poly (vinyl alcohol)-g-poly (acrylic acid) hydrogels impregnated with polyaniline. eXpress Polym. Lett. 2008; 2: 26-39.
47. Narbat MK, Hashtjin MS, Pazouki M. Fabrication of porous hydroxyapatite-gelatin scaffolds crosslinked by glutaraldehyde for bone tissue engineering. Iran J. Biotechnol. 2006; 4: 54-60.
48. Pradeesh TS, Sunny MC, Varma HK. Ramesh P. Preparation of microstructured hydroxyapatite microspheres using oil in water emulsions. Bull. Materl. Sci. 2005; 28: 383-390.
49. Kalasin S, Santore MM. Non-specific adhesion on biomaterial surfaces driven by small amounts of protein adsorption.Colloids Surfaces B: Biointerfaces. 2009; 73: 229-236.
50. Akaike T, Okano T, Terano M, Yui N. Adv. Polym. Biomaterl. Sci, CMC Co. Ltd.: Tokyo, (1997).